Energy harvesting by two magnetopiezoelastic oscillators with mistuning

Grzegorz Litak,[1, a)] Michael I. Friswell,[2] Cedrick A. Kitio Kwuimy,[3] Sondipon Adhikari,[2] and Marek Borowiec[1]

[1)] *Department of Applied Mechanics, Technical University of Lublin, Lublin PL-20-618, Poland*
[2)] *School of Engineering, Swansea University, Singleton Park, Swansea SA2 8PP, UK*
[3)] *Center for Nonlinear Dynamics and Control, Department of Mechanical Engineering, Villanova University, 800 Lancaster Avenue, Villanova, PA 19085, USA.*

Abstract We examine an energy harvesting system of two magnetopiezoelastic oscillators coupled by electric circuit and driven by harmonic excitation. We focus on the effects of synchronization and escape from a single potential well. In the system with relative mistuning in the stiffness of the harvesting oscillators, we show the dependence of the voltage output for different excitation frequencies. © 2012 *The Chinese Society of Theoretical and Applied Mechanics.* [doi:10.1063/2.1204309]

Ambient energy harvesting by autonomous electromechanical systems is an important source of energy for small electronic devices and to recharge batteries or enable remote operation.[1,2] Many of the proposed devices use the piezoelectric and electrostatic effects as the transduction method.[3–6] These devices are usually implemented as patches on cantilever beams and designed to operate at resonance conditions. The design of an energy harvesting device must be tailored to the ambient energy available. For a single frequency excitation the resonant harvesting device is optimum, provided it is tuned to the excitation frequency.[7,8]

To optimize the harvesting system for harmonic excitation, the harvester is designed with a natural frequency to match the excitation frequency.[1,7] For harmonic excitation where the frequency varies, or for broadband excitation, the bandwidth of the device has to be extended. Nana and Woafo[9] suggested the use of an array of two or more harvesters to increase the power delivered into the load. Shahruz[10] analyzed a set of parallel single degree of freedom harvesters tuned at slightly different resonant frequencies, whereas Erturk et al.[11] considered a harvester as a serial set of two beams connected to each other to form an L-shape. Ferrari et al.[12] investigated a piezoelectric multifrequency energy converter for power harvesting in autonomous microsystems. Ramlan et al.[13] considered a harvester made of two oblique springs and analyzed the potential benefits of the hardening effects of the spring on the output energy.

More recently Kim et al.[14] introduced the idea of association of two piezoelectric harvesters to produce more efficient electric power generation. Their model consisted of a proof mass, two cantilever piezoelectric beams delivering the electric signal into an electrical load. They showed through experimental analysis that a two degrees of freedom energy harvester has two peaks at different frequencies and also has a large frequency bandwidth in comparison with the conventional single degree of freedom piezoelectric harvester. As suggested by Kim et al.,[14] connecting energy sources do not necessarily result in an increase in the power generated. Therefore a rigorous mathematical analysis has to be performed to analyze the synchronization condition of the harvesters.

The above discussion highlights the current requirement for energy harvesting solutions from broadband vibration. Nonlinear dynamic systems have shown potential to deliver novel broadband harvesting solutions. However a full understanding of the nonlinear dynamics of these systems is required. This letter considers a candidate energy harvesting solution based on two magnetopiezoelastic beams delivering power into an electrical circuit. A novel analysis is provided for the mistuning in the stiffness of the harvesting oscillators, which is vital to provide a broadband response but significantly complicates the resulting analysis.

A schematic picture of the parallel coupled harvesters is shown in Fig. 1(a). The mathematical model may be written as the following dimensionless equations

$$\ddot{x} + 2\zeta\dot{x} - \frac{1}{2}x(1 - x^2) - \chi v = F(t),$$
$$\ddot{y} + 2\zeta\dot{y} - \frac{1}{2}\alpha y(1 - y^2) - \chi v = F(t), \qquad (1)$$

and

$$\dot{v} + \lambda v + \kappa\dot{x} + \kappa\dot{y} = 0, \qquad (2)$$

where x and y are the dimensionless transverse displacements of the beam tips, v is the dimensionless voltage across the load resistor, χ is the dimensionless piezoelectric coupling term in the mechanical equation, κ is the dimensionless piezoelectric coupling term in the electrical equation, $\lambda \propto 1/RC_{\mathrm{P}}$ is the reciprocal of the dimensionless time constant of the electrical circuit, R is the load resistance, and $C_{\mathrm{P}} = C_{\mathrm{P1}} + C_{\mathrm{P2}}$ is the capacitance of the piezoelectric material. Finally, α is the stiffness mistuning parameter which should be considered in any

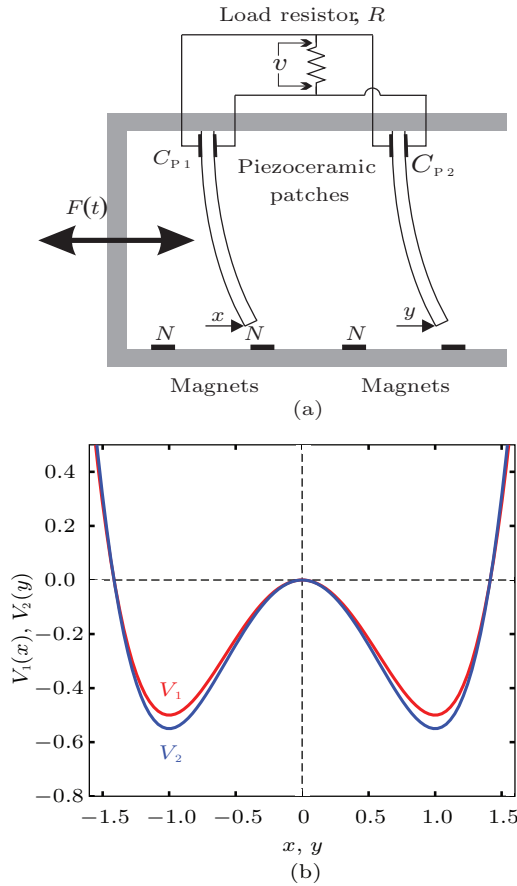a)Corresponding author. Email: g.litak@pollub.pl.

(a)

(b)

Fig. 1.   (a) Schematic diagram of the harvester system; (b) Potentials of restore forces $V_1(x) = -x^2 + x^4/2$ and $V_2(y) = \alpha(-y^2 + y^4/2)$ ($\alpha = 1.1$) against displacements x and y for the corresponding mechanical oscillators (Eq. (1)).

(a)

(b)

Fig. 2. (a) Output power in terms of mean squared voltage $\langle v^2 \rangle$ versus excitation frequency ω; (b) Relative difference in the oscillator displacements $x - y$ in terms standard deviation $\sigma(x - y)$ versus excitation frequency ω. In the simulations the frequency was changed quasi-statically (the system parameters are given in Eq. (4)).

realistic system, and $F(t)$ is the harmonic excitation of the following form

$$F(t) = F_0 \sin(\omega t). \tag{3}$$

The double well potentials of the proposed mechanical oscillators (Fig. 1(a), Eq. (1)) are shown in Fig. 1(b).

Using the above equations (Eqs. (1)–(3)) we performed simulations of the dynamical system. The system parameters used in the calculations were chosen to fit a realistic experiment[7]

$$\chi = 0.05, \quad \kappa = 0.5, \quad \lambda = 0.01,$$
$$\zeta = 0.01, \quad F_0 = 0.2, \quad \alpha = 1.1. \tag{4}$$

The results of the output power as well as the appearance of synchronization are illustrated in Fig. 2. As expected the resonance curve mirrors the mechanical hardening. Duffing type nonlinearity and the peak frequency is located at about $\omega \approx 1.0$ (Fig. 2(a)). Interestingly, after passing through the maximum response the system switches from the resonant to the non-resonant solution. By examining the standard deviation of oscillator's relative displacement $\sigma(x-y)$ we observe that the
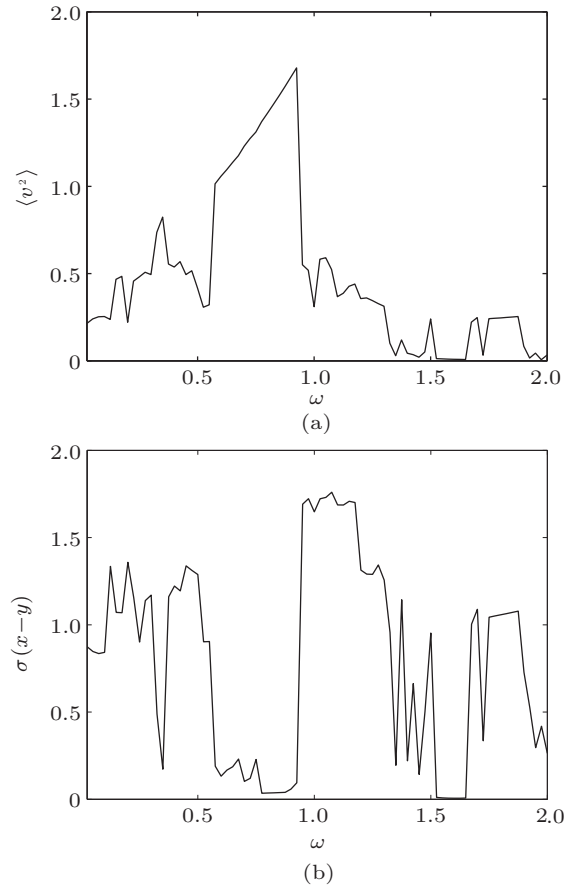
mistuning parameter $\alpha = 1.1$ breaks the synchronization effect (Fig. 2(b)). Synchronization ($\sigma(x - y) \approx 0$) is fulfilled for $\omega \in [0.60, 0.95]$ and $[1.55, 1.60]$. Interestingly, the resulting power generated in the second interval is low. However at frequency giving the peak power $\sigma(x - y) \approx 1.6$.

To investigate the above solutions of Eqs. (1)–(3) further, Fig. 3 shows the simultaneously estimated average values of $\langle x \rangle$ and $\langle y \rangle$. By observing these parameters one can distinguish the symmetric (usually doublewell) and non-symmetric (usually single-well) solutions. Apart from some synchronized motions where both averages ($\langle x \rangle$ and $\langle y \rangle$) have fairly close values, there are also regions with completely different averages. It is evident that mistuning (see α in Eq. (1)) can lead to complicated mixed solutions where one of the oscillators exhibits single well vibrations while the other exhibits double-well vibrations.

The effect of switching between different possible solutions, from single to double well solutions and vice versa, can be also identified in Fig. 4, where we present the bifurcation diagrams for the mistuned oscillators.
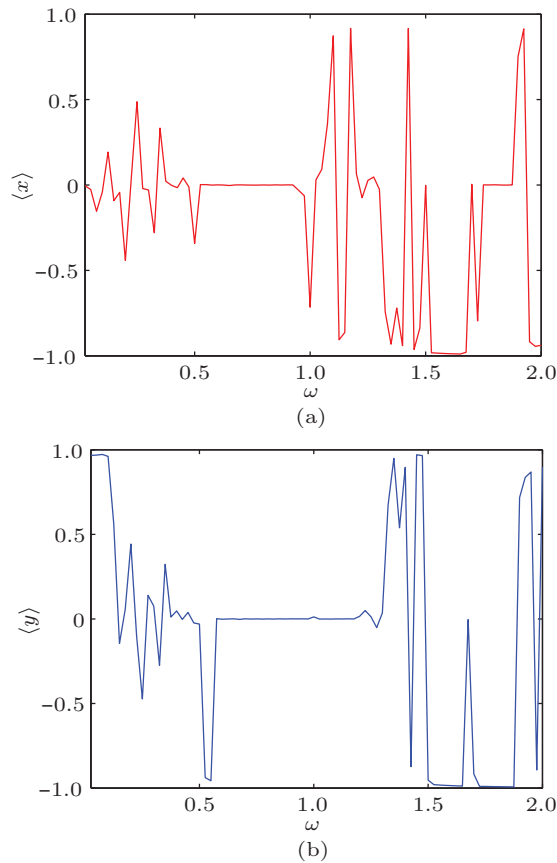
Fig. 3. The average values of x and y displacements: (a) $\langle x \rangle$, (b) $\langle y \rangle$ versus excitation frequency ω, obtained simultaneously with results in Fig. 2.

Fig. 4. Simultaneously estimated bifurcation diagrams for (a) x, and (b) y versus the excitation frequency ω, which was changed quasi-statically (the system parameters are shown in Fig. 2).

For more detailed studies we have concentrated on the three cases defined by different excitation frequency $\omega = 0.75$, 1.00, 1.70. The corresponding phase portraits, Poincare points and time series are illustrated in Figs. 5–7, respectively. The initial conditions were chosen as $[x, \dot{x}, y, \dot{y}, v] = [0.01, 0, 0.01, 0, 0]$ for each case.

Note that according to Fig. 2(b) the solution for $\omega = 0.75$ is fairly well synchronized. The topology of phase portraits and Poincare maps (Figs. 5(a), 5(c)) and the simultaneous time series (Figs. 5(b), 5(d)) confirm that conclusion. Interestingly the system response period corresponds to four excitation periods which is presumably due to the electrical coupling of mechanical parts (Eqs. (1) and (2)) and the effect of mistuning (Fig. 1(b)).

The solution for $\omega = 1.00$ is obviously non-synchronized (see Fig. 2(b)). Note that Figs. 6(c), 6(d) clearly show that the discussed solution is chaotic. Interestingly, the chaotic solution seems to be induced by the second oscillator (with the coordinate y) while the first oscillator (with the coordinate x) shows a more regular response (Figs. 4(a), 4(b)). In the plane x–$\dot{x}$, the attractor (Fig. 4(a)) resembles a smeared point of a regular solution in the presence of noise-like disturbances. These disturbances are created by the chaot-
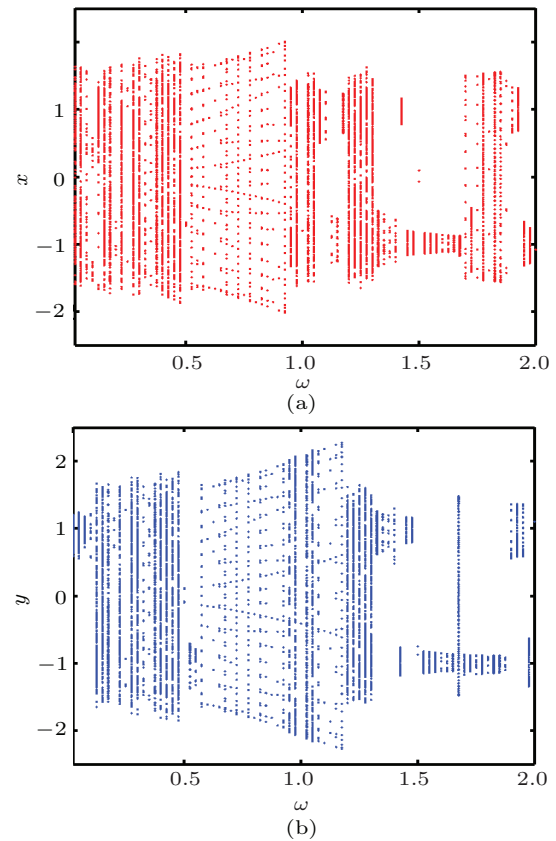
ically changing coordinate y coupled to the first oscillator through the linear electrical circuit coupling (Eq. (2)).

Finally, the solution for $\omega = 1.70$ shows interesting phenomena and the corresponding phase portraits show a different topology. The first mechanical beam structure oscillates in a single potential well (Figs. 7(a), 7(b)) while the second beam structure exhibits well developed oscillations (Figs. 7(c), 7(d)) crossing the potential well $V_2(y)$ (Fig. 1(b)). This phenomenon is related to the nonuniform distribution of the system energy. The above solutions confirm qualitatively the appearance of different averages $\langle x \rangle$ and $\langle y \rangle$ shown in Fig. 3 in the region of $\omega \in [1.75, 1.90]$, as well as the differences in the bifurcation diagram. However one should note that different initial conditions may lead to different solutions and consequently change the vibrational energy concentration in this nonlinear system. From the Poincare points one can conclude that the response frequency corresponds to thirty excitation periods.

In summary, we have investigated the dynamical response of two magnetopiezoelastic harvesters with mistuned stiffness connected in a parallel way via an electrical circuit. The total output power versus the excitation frequency showed the typical resonance curve, however
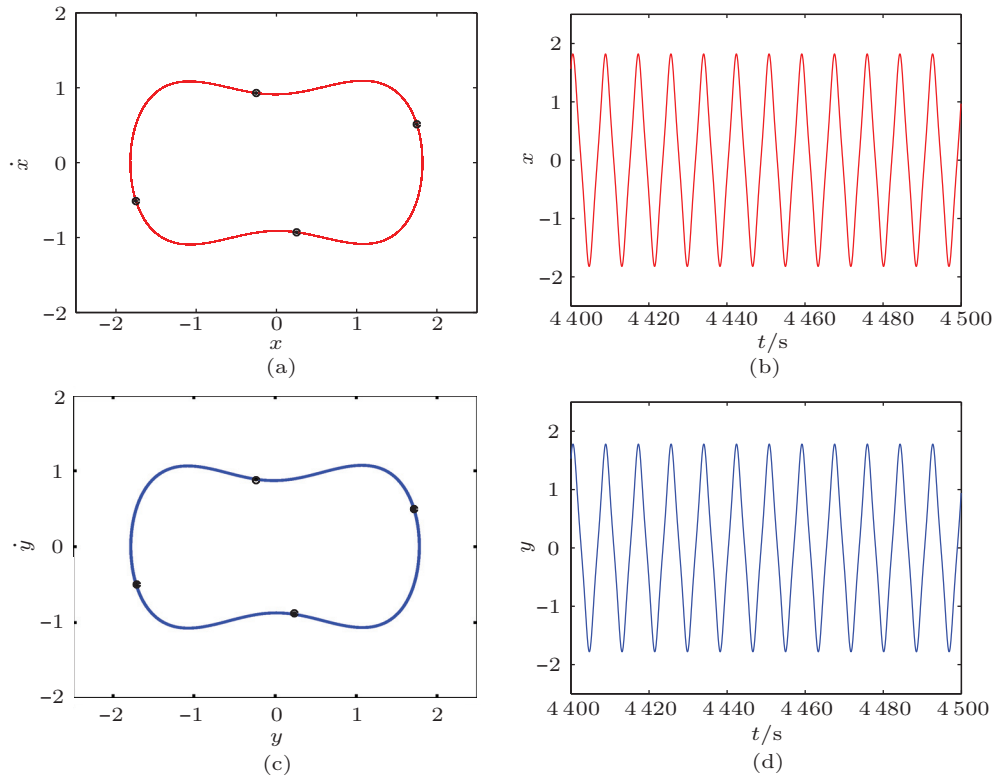
Fig. 5.   Phase portraits (lines) with Poincare points (black points) projected into planes x–$\dot{x}$ in (a) and y–$\dot{y}$ in (c), and time series of $x(t)$ in (b) and $y(t)$ in (d) for $\omega = 0.7$.
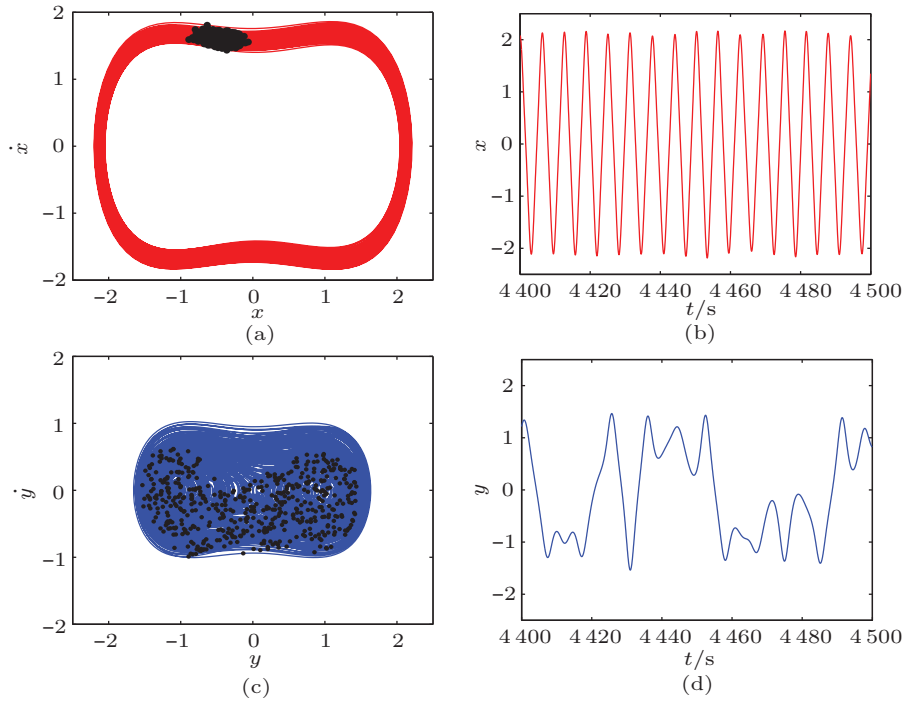

Fig. 6.   Phase portraits (lines) with Poincare points (black points) projected into planes x–$\dot{x}$ in (a) and y–$\dot{y}$ in (c), and time series of $x(t)$ in (b) and $y(t)$ in (d) for $\omega = 1$.
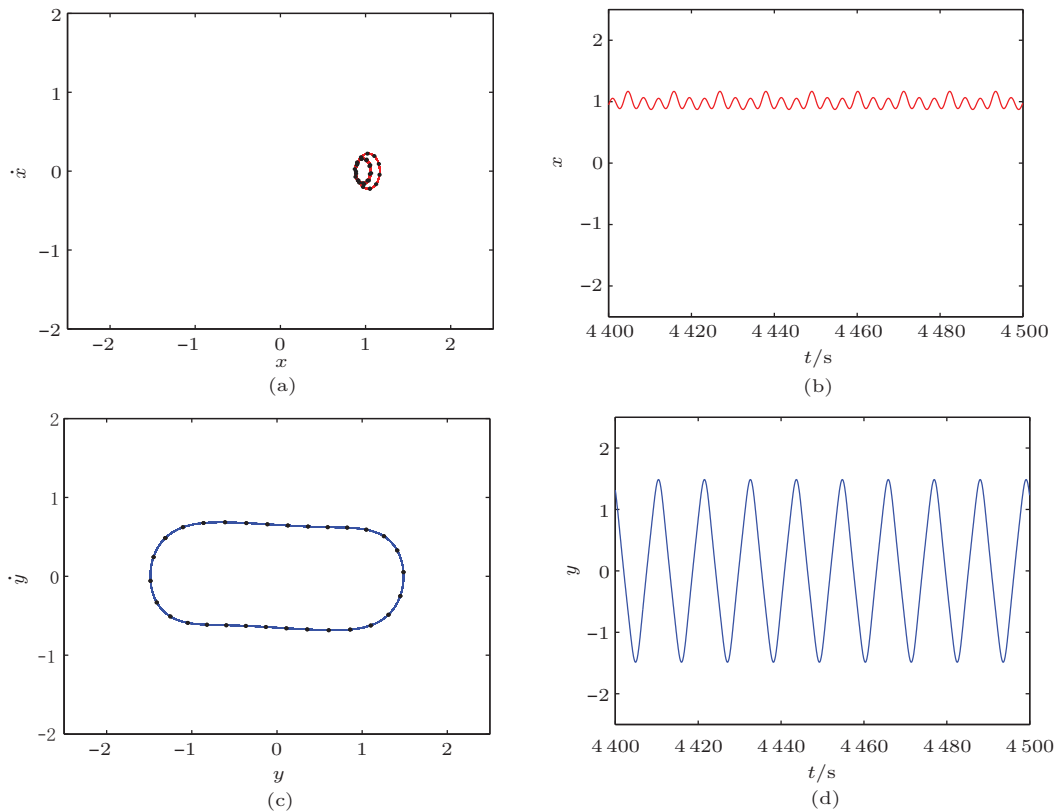
Fig. 7. Phase portraits (lines) with Poincare points (black points) projected into planes x–$\dot{x}$ in (a) and y–$\dot{y}$ in (c), and time series of $x(t)$ in (b) and $y(t)$ in (d) for $\omega = 1.75$.

due to mistuning the harvesters worked mostly in the unsynchronized regime. In the vicinity of the resonance peak we found a chaotic solution which was driven by one of the oscillators.

Note that in this paper we used only one set of initial conditions (Figs. 5–7) and ω was changed quasi-statically (to get the results in Figs. 2–4). However, to explain the problem of multiple solutions in nonlinear systems (Eqs. (1)–(3)) their synchronization, and bifurcations one has to perform more extended studies on initial conditions and to estimate basins of attraction for the given excitation frequency ω. For instance, two degrees of freedom dynamical systems with friction have been extensively studied by Awrejcewicz and Olejnik.[15,16]

It is interesting that the appearance of different solutions directly affect the energy harvesting as they implies various distributions of the vibrational energy. Furthermore, it would be important to note to test the robustness of particular solutions against weak noise conditions.[5,17]

1. A. Erturk, and D. J. Inman, *Piezoelectric Energy Harvesting* (Wiley, Chichester, 2011).
2. S. R. Anton, and H. A. Sodano, Smart Mater. Struct. **16**, R1 (2007).
3. D. P. Arnold, IEEE Trans. Magn. **43**, 3940 (2007).
4. S. P. Beeby, R. N. Torah, and M. J. Tudor, et al., J. Micromech. Microeng. **17**, 1257 (2007).
5. G. Litak, M. I. Friswell, and S. Adhikari, Appl. Phys. Lett. **96**, 214103 (2010).
6. M. Lallart, S. Pruvost, and D. Guyomar, Phys. Lett. A **375**, 3921 (2011).
7. A. Erturk, J. Hoffmann, and D. J. Inman, Appl. Phys. Lett. **94**, 254102 (2009).
8. S. C. Stanton, C. C. McGehee, and B. P. Mann, Physica D **239**, 640 (2010).
9. B. Nana, and P. Woafo, Physica A **387**, 3305 (2008).
10. S. M. Shahruz, J. Sound Vib. **292**, 987 (2006).
11. A. Erturk, J. M. Renno, and D.J. Inman, J. Intell. Mater. Syst. Struct. **20**, 529 (2009).
12. M. Ferrari, V. Ferrari, and M. Guizzetti, et al., Sens. Actuators A **142**, 329 (2008).
13. R. Ramlan, M. Brennan, and B. Mace, et al., Nonlinear Dyn. **59**, 54 (2010).
14. I. Kim, H. Jung, and B. M. Lee, et al., Appl. Phys. Lett. **98**, 214102 (2011).
15. J. Awrejcewicz, and P. Olejnik, Int. J. Bif. Chaos **13**, 843 (2003).
16. J. Awrejcewicz, and P. Olejnik, Int. J. Bif. Chaos **15**, 1931 (2005).
17. G. Litak, M. Borowiec, and M. I. Friswell, et al., J. Theor. Appl. Mech. **49**, 757 (2011).